N O T I C E

THIS DOCUMENT HAS BEEN REPRODUCED FROM MICROFICHE. ALTHOUGH IT IS RECOGNIZED THAT CERTAIN PORTIONS ARE ILLEGIBLE, IT IS BEING RELEASED IN THE INTEREST OF MAKING AVAILABLE AS MUCH INFORMATION AS POSSIBLE

NASA

# Technical Memorandum 82043



# System Calibration of the 1.4 GHz and 5 GHz Radiometers for Soil Moisture Remote Sensing

**J. Wang, J. Shiue, W. Gould, J. Fuchs,**

**E. Hirschmann, and W. Glazar**

**NOVEMBER 1980**

National Aeronautics and
Space Administration

**Goddard Space Flight Center**
Greenbelt, Maryland 20771

**Page intentionally left blank**

TM 82043

# SYSTEM CALIBRATION OF THE 1.4 GHz AND 5 GHz RADIOMETERS FOR SOIL MOISTURE REMOTE SENSING

By

J. Wang, J. Shiue, W. Gould, J. Fuchs,
E. Hirschmann, and W. Glazar
Earth Observation Systems Division

November 1980

GODDARD SPACE FLIGHT CENTER
Greenbelt, Maryland 20771

# SYSTEM CALIBRATION OF THE 1.4 GHz AND 5 GHz RADIOMETERS FOR SOIL MOISTURE REMOTE SENSING

By
J. Wang, J. Shiue, W. Gould, J. Fuchs,
E. Hirschmann, and W. Glazar
Earth Observation Systems Division

## ABSTRACT

Two microwave radiometers at the frequencies of 1.4 GHz and 5 GHz were mounted on a mobile tower (Cherry Picker) and used for remote sensing of soil moisture experiment at a Beltsville Agriculture Research Center's test site. The experiment was performed in October 1979 over both bare field and fields covered with grass, soybean, and corn. This document describes the calibration procedure for the radiometer systems which forms the basis of obtaining the final radiometric data product. Based on the calibration results, it is estimated that the accuracy of the 1.4 GHz radiometric measurements is about ±3°K. The measured 5 GHz brightness temperatures over bare fields with moisture content >10% by dry weight are about 8°K lower than those taken simultaneously at 1.4 GHz. This could be due to either 1) a 5 GHz antenna side lobe seeing the cold brightness of the sky, or 2) the thermal microwave emission from a soil being less sensitive to surface roughness at 5 GHz than at 1.4 GHz.

Measurements on the effect of radiometers' self-emission are also made over a smooth water surface. It is concluded from these measurements that the data collected over all fields at incident angle $\theta = 0^\circ$ are contaminated by radiometers' self-emitted energy backscattered from the ground. For $\theta \geq 10^\circ$ this self-emission effect is negligible if the radiometers are maintained at a height greater than 3 m above the ground.

# SYSTEM CALIBRATION OF THE 1.4 GHz AND 5 GHz RADIOMETERS FOR SOIL MOISTURE REMOTE SENSING

## 1. INTRODUCTION

Remote measurements of soil moisture content by truck-mounted microwave radiometers have been carried out in the past few years by Newton (1975), Newton and Tesch (1976), and by Njoku and Kong (1977). The Measurements by Newton, and Newton and Tesch were made over both bare and vegetated fields with 1.4 GHz (L-band) and 10.7 GHz (X-band) radiometers. The soil type was Miller clay and the vegetation covers were sorghum hybrid and cotton. The measurements by Njoku and Kong were limited to bare fields of sandy soils and the results given in their report covered the frequencies of 10.7 GHz and 30 GHz only. Clearly more measurements are needed in order to understand the various parameters (e.g., moisture content, surface roughness, soil type, and vegetation cover, etc.) which affect the microwave emission from soils. For this reason, two radiometers at 1.4 GHz and 5 GHz (C-band) frequencies were mounted on a truck and radiometric measurements were made over both bare fields and fields covered with grass, soybean, and corn at a Beltsville Agricultural Research Center's test site. The details of the field description and experimental results were given in a report by Wang et al. (1980).

The objective of this document is to provide a detailed description of the radiometer systems' calibration procedure as well as the problems encountered in the systems' operation. Based on the calibration data, an assessment is made on the accuracy of the radiometric measurements. The effect of the radiometers' self-emission, which was observed previously by Carver (1978) and Newton (personal communication) was measured over a smooth water surface. The impact of this effect

on the field radiometric measurements by both L- and C-band radiometers at height $\gtrsim$ 3 m was shown to be negligible for incident angles $\geq$ 10°. The measured C-band brightness temperatures over bare fields were found to be lower than the corresponding L-band values more than 60% of the times. Comparisons among the measured data sets, including both calibration and field radiometric measurements, indirectly showed that the C-band antenna might be the cause of the measured low brightness temperatures.

## 2. EXPERIMENT SYSTEMS

Both the L-band and C-band radiometers are of the Dicke type which measure the target radiometric responses in both vertical and horizontal polarizations simultaneously. The L-band radiometer has a 1.22-m dish antenna which gives a 3 db beamwidth of ~12°. The 5 GHz radiometer antenna is a 0.8 m x 0.8 m slotted waveguide phased array and has a 3 db beamwidth of ~8°. Figures 1 and 2 show the vertically polarized radiation patterns for the L-band and C-band antenna respectively. Similar patterns for both bands were also observed for the horizontal polarization. Only a single-cut antenna pattern measurement was made at each polarization for either radiometer. Therefore, it is difficult to estimate the percent contribution from the side lobes to the radiometric measurements. Both radiometers were mounted on a platform at the top of a cherry picker boom and were maintained at ~6 m above ground during measurements when incident angle $\theta$ was $\leq$30°. An inclinometer was attached to the platform for precision measurements of $\theta$ which were fed to a Hewlett-Packard (HP) 9835 desktop calculator for verification.

The HP desktop calculator is the main component of the data system used in the microwave sensor operation. It sends out commands to the radiometers to dwell on a particular mode (i.e., hot load, cold load, or antenna port) and receives signals from the radiometers for real time.

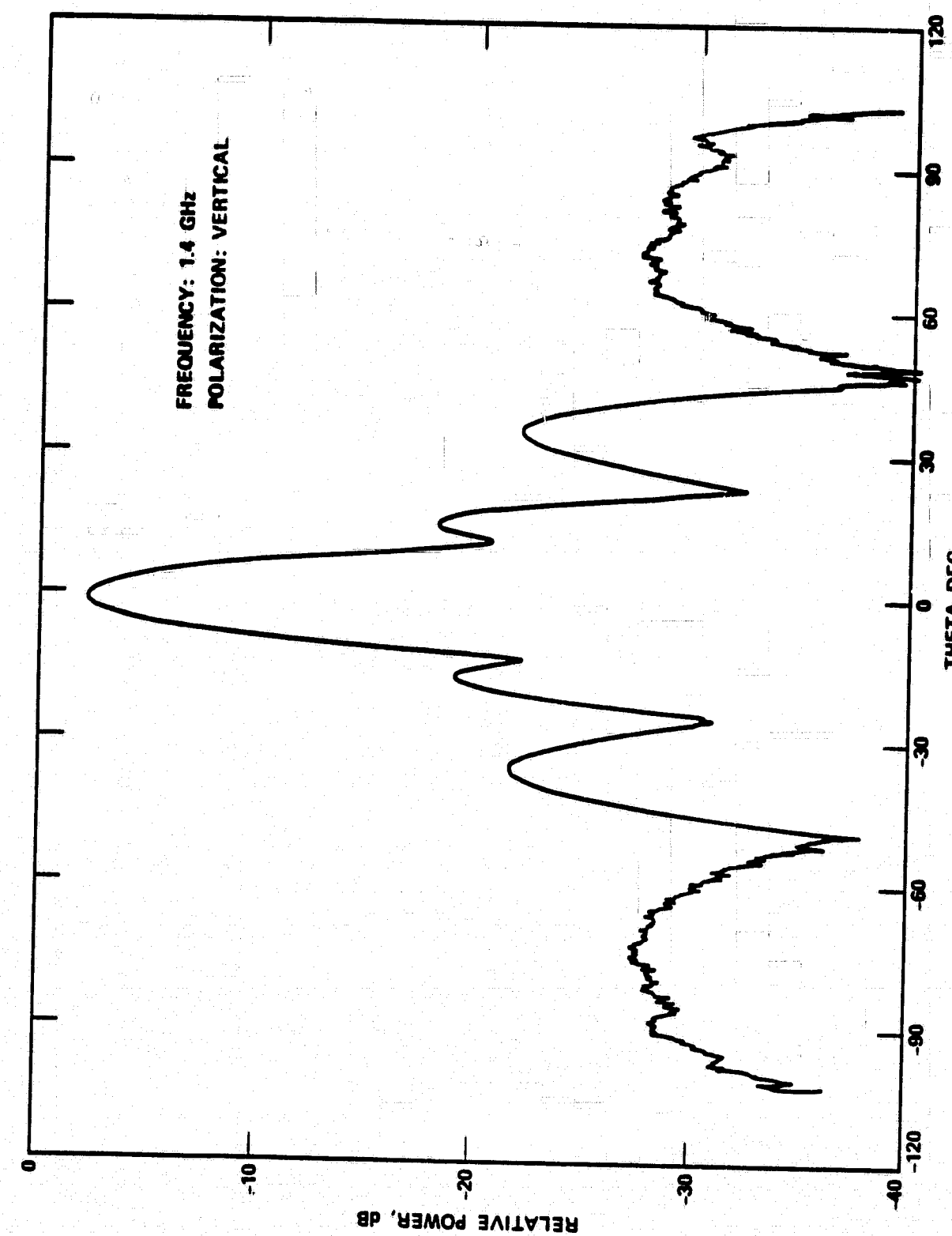


Figure 1. The measured radiation pattern for the L-band dish antenna (vertical polarization).

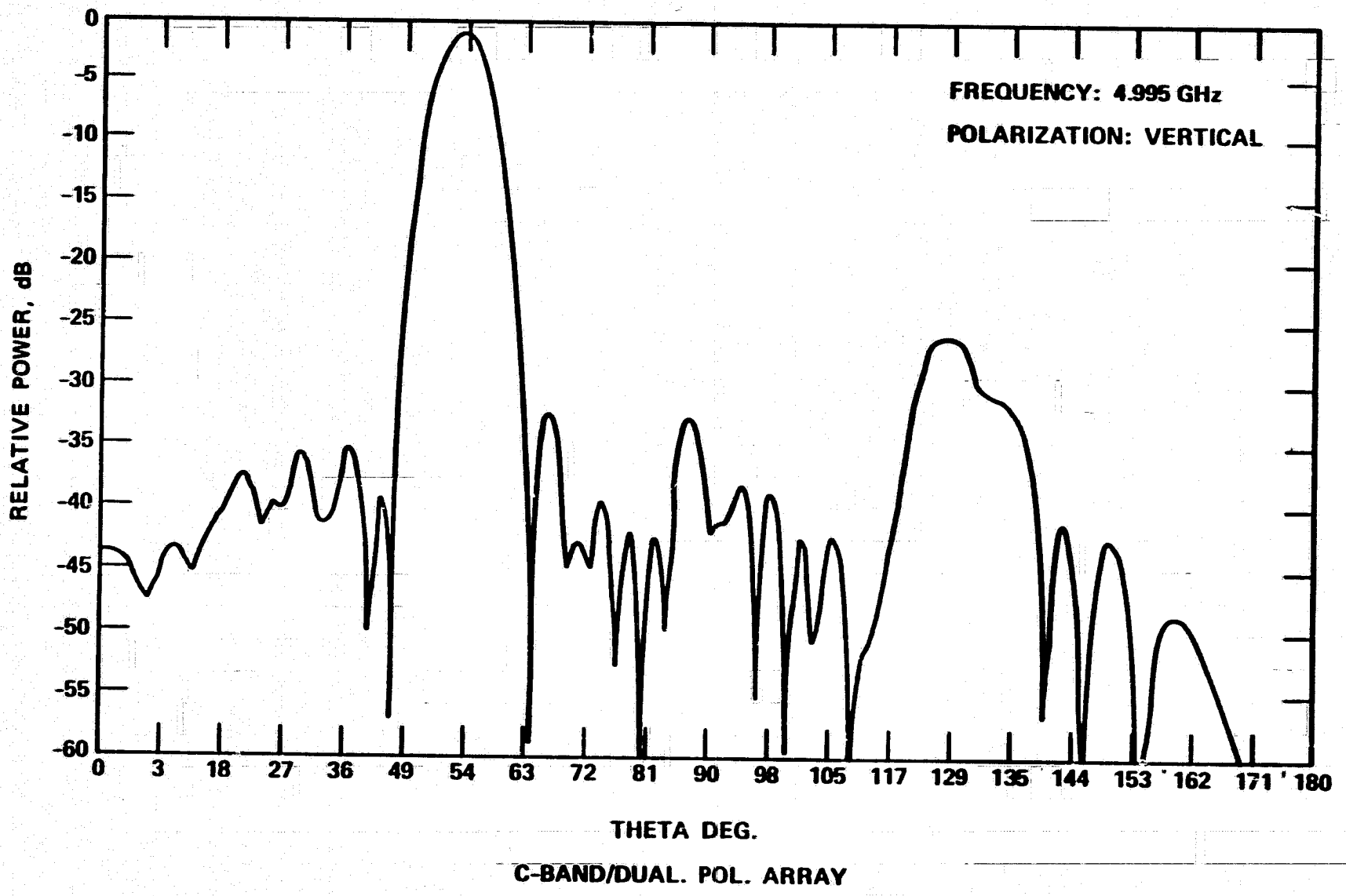


Figure 2. The measured radiation pattern for the C-band phased array antenna (vertical polarization).

processing and data recording. In addition to the calculator, the data system also includes an HP scanner and an HP digital voltmeter. The scanner has a 48-channel capacity and, upon receiving commands from the calculator, selects a particular channel (e.g., voltage signals from L-band or C-band radiometer and various housekeeping data) for data input to the calculator. The digital voltmeter provides measurements of incoming antenna signals as well as housekeeping data.

There are two internal calibration references for each of the radiometer system: a hot load at 300°K and a cold load at the liquid nitrogen temperature of 77°K. During the radiometric measurements, the incoming signals are compared with these reference loads so that normalized signal voltages independent of gain drift are obtained. From these normalized voltages, the brightness temperatures of various targets are determined from the calibration equations described below.

## 3. SYSTEM CALIBRATION

### A. Calibration Procedures and Targets

The calibration procedures of both C-band and L-band radiometers were discussed in detail in the report of Wang et al. (1980). Basically it was assumed that the measured brightness temperature $T_{BP}$ is linearly related to the normalized antenna voltage $N_P$, i.e.,

$$T_{BP} = aN_P + b \tag{1}$$

where the subscript P stands for either vertical or horizontal polarization. a and b are coefficients which can be determined by pointing the antenna at the targets of known brightness temperature response. $N_P$ is related to the measured antenna voltage of the target $V_P$, cold load voltage $V_c$ and hot load voltage $V_h$ by

$$N_P = \frac{V_P - V_h}{V_c - V_h} \qquad (2)$$

Three known targets were used for the radiometer calibration: sky, Eccesorb slab, and smooth water surface. The response of these targets is briefly described below.

a. Sky. Most of the radiometer calibrations during the period of soil moisture measurements were performed when the sky was clear. At the frequencies of 1.4 GHz and 5 GHz the atmosphere is not lossy in the absence of heavy clouds. The brightness temperatures of the sky seen by the ground radiometers at these frequencies can be regarded as constants derivable from the standard atmosphere model calculation. Assuming an integrated water vapor content in the atmosphere of 3.5 cm, the $T_B$'s for sky at 1.4 GHz and 5 GHz calculated from the U.S. Standard Atmosphere Model were 4.89°K and 5.36°K respectively. A change in the integrated column of water vapor to 1.9 cm gave the corresponding change in the sky $T_B$'s to 4.88°K and 5.22°K at the same frequencies which was not significant indeed. The values of 4.89°K at 1.4 GHz and 5.36°K at 5 GHz were used as a standard in the system calibration.

b. Eccosorb slabs. Each piece of Eccosorb slab (absorption coefficient of 0.99) used in the radiometer calibration has a size of 61 cm x 61 cm x 23 cm. Twelve pieces of identical Eccosorb slabs were placed on the ground (with grass cover) giving enough area to perform calibration of both radiometers simultaneously. The radiometer antennas were placed as close as possible to the Eccosorb slabs in the calibration. The physical temperature of the Eccosorb slabs was measured at three different locations and the average value was used in the calibration. The same calibration procedure was used in all the field measurements.

c. Smooth Water Surface. The brightness temperature of fresh water can be estimated fairly accurately, knowing the water physical temperature and salinity content (Paris, 1969). Wilheit (personal communication) had derived a set of formulas from the curve fitting to the data of Lane and Saxton (1952) for the water brightness temperature calculations. The contribution from the reflection of sky brightness temperature at the water surface was added to obtain the final water brightness temperature used in the calibration.

The water calibration measurements were made on October 17 and 18 of 1979 at a two-acre pond inside Goddard Space Flight Center. Only the measurements at incident angles $\theta$ ranging from 10° to 60° were used for the system calibration. The measurements at $\theta = 0°$ were discarded because of the systems' self-emission problem to be discussed in Section 5.

## B. Calibration Results

Results of the system calibration were shown in Figures 3 and 4 for C-band and L-band radiometers respectively. In both figures the measured or computed brightness temperatures of sky, Eccosorb slabs, and smooth water surface were plotted against the corresponding normalized radiometer output voltages. To avoid crowding the plots in the ~5°K region, three to four measured values in the sky calibration were averaged and only the averaged results were shown. There were two distinct features displayed by the data in these figures. First, both C-band and L-band radiometers showed a linear response over the entire brightness temperature region of interest. Secondly, over the consecutive days of water calibrations when the water temperatures were ~16.5° and ~17°C, both radiometers demonstrated a repeatability of measurements in both vertical and horizontal polarizations.

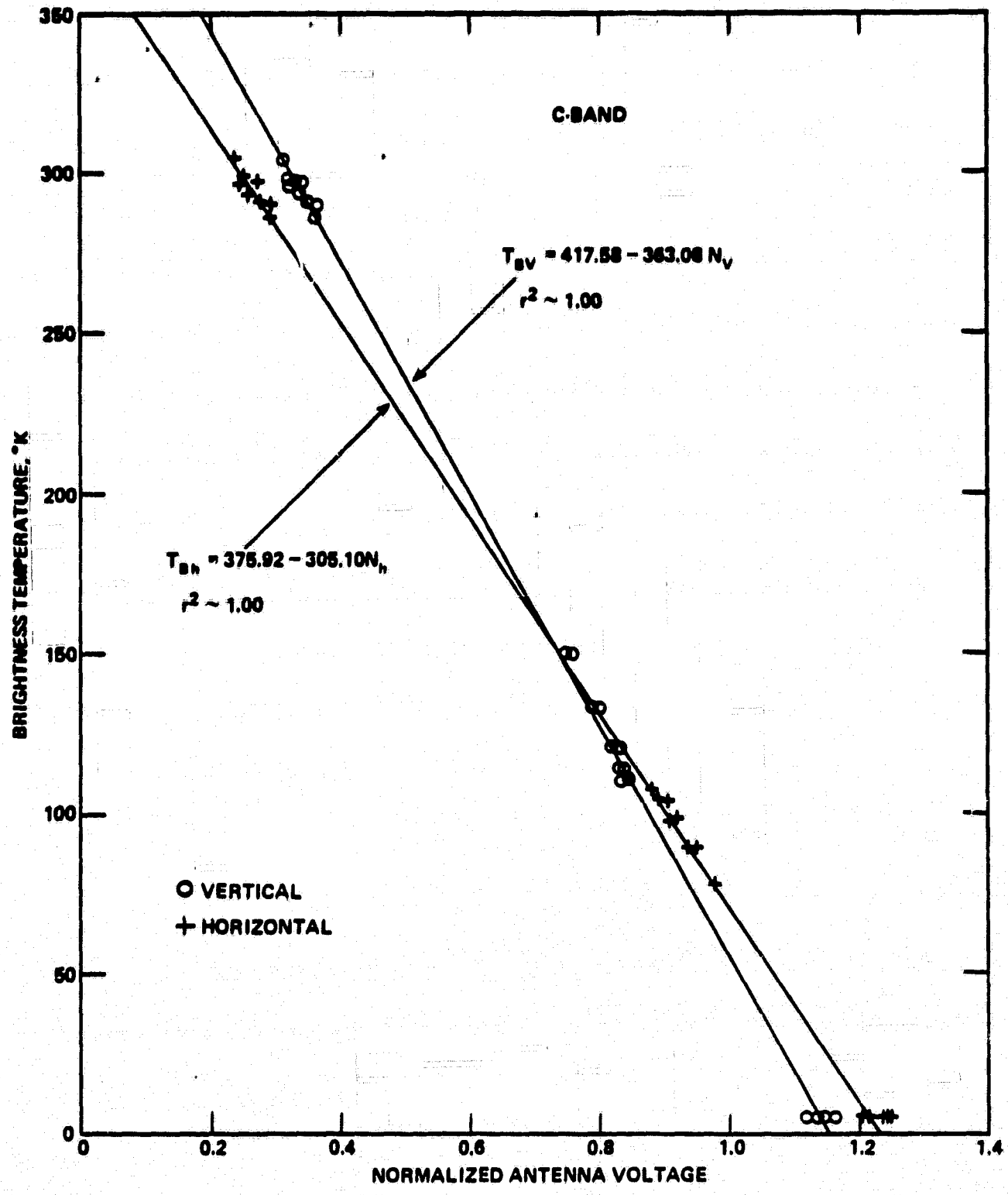


Figure 3. The C-band calibration data and results.

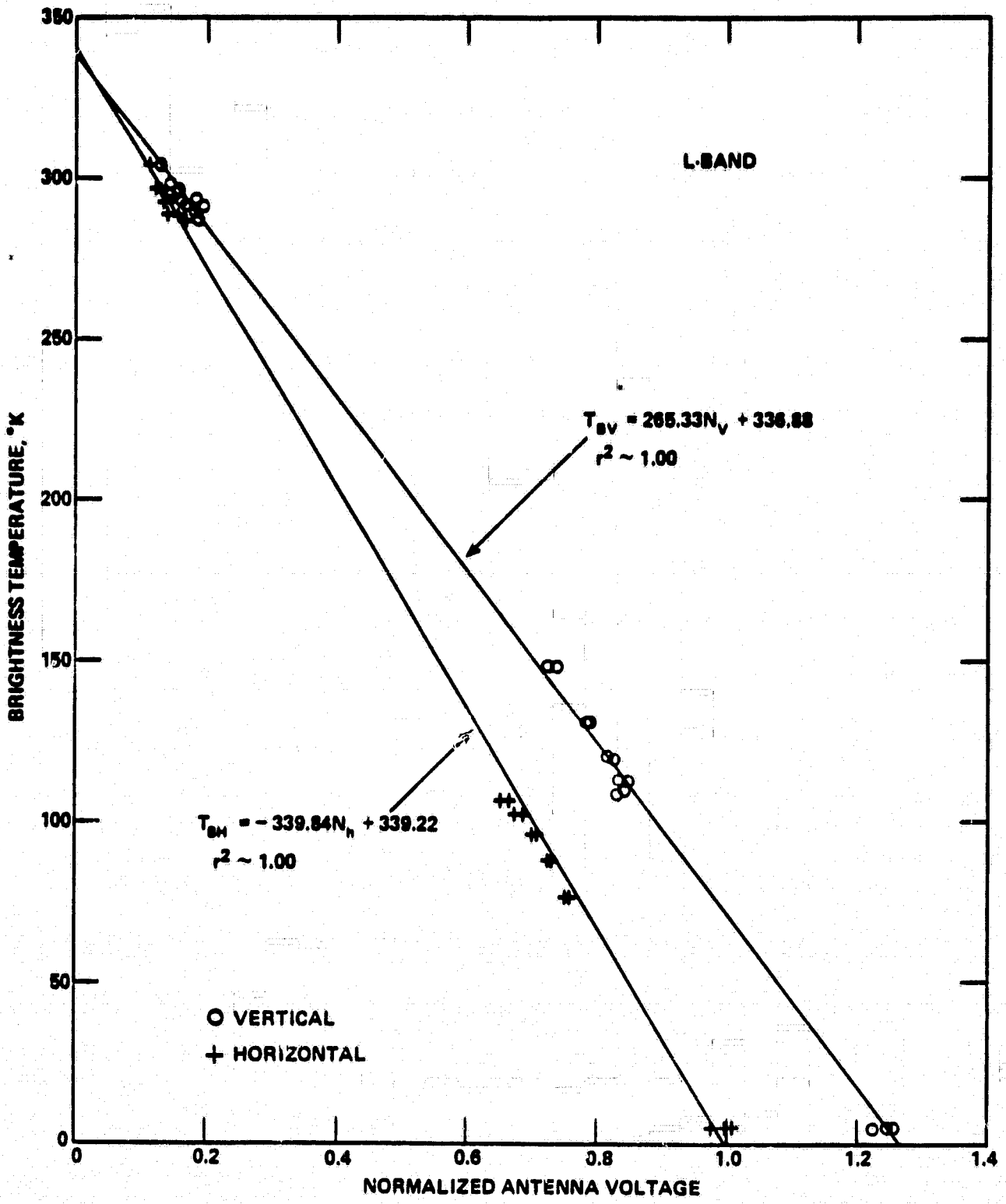


Figure 4. The L-band calibration data and results.

A linear regression was applied to each of the four data sets (two frequencies and two polarizations). The resultant expressions for the brightness temperatures are

for C-band:

$$T_{BV} = 417.58 - 363.08\, N_V \quad (3)$$

$$T_{BH} = 375.92 - 305.10\, N_H \quad (4)$$

and for L-band:

$$T_{BV} = 336.88 - 265.33\, N_V \quad (5)$$

$$T_{BH} = 339.22 - 339.84\, N_H \quad (6)$$

In all four cases of regression analysis, the correlation coefficient is ~1.

To see whether there is a systematic drift in the day-to-day calibration measurements, the temperature difference $\Delta T$'s are taken between the known brightness temperature $T_B$'s of the Eccosorb slabs and sky and the corresponding $T_B$'s calculated from Equations (3) through (6) with measured $N_V$ and $N_H$. The resultant $\Delta T$'s were plotted against the date of measurements in Figures 5 and 6 for C-band and L-band radiometers respectively. For Eccosorb calibration, there is no systematic drift in $\Delta T$ with time for both radiometers. The average fluctuation from the mean $\Delta T$ for either radiometer is ~ $\pm 2^\circ$K. For the sky calibration, while again there is no systematic drift in $\Delta T$ for both radiometers, the excursion of $\Delta T$ from the mean value for C-band radiometer was clearly much bigger compared to the case for Eccosorb calibration.

## 4. SOME MEASUREMENT RESULTS

Figure 7 shows a set of measurement results over a bare field with a fairly uniform moisture of value ~22% down to ~10 cm. Both C-band and L-band brightness temperatures $T_B$'s are obtained using calibration equations (3) through (6). Note that $T_B$'s for C-band are lower than those for

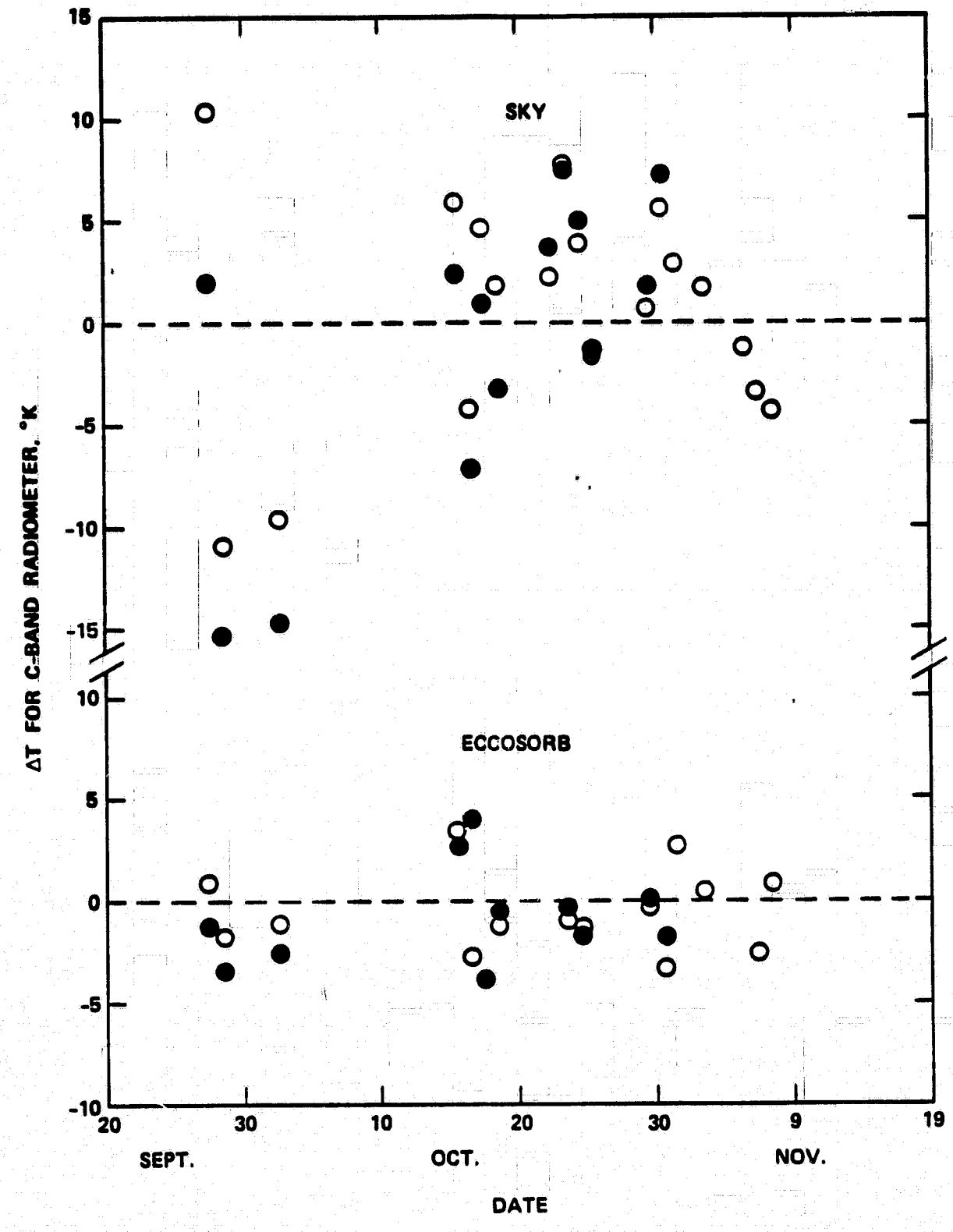


Figure 5. The difference between the measured and calculated C-band brightness temperatures for two calibration targets plotted as a function of time.

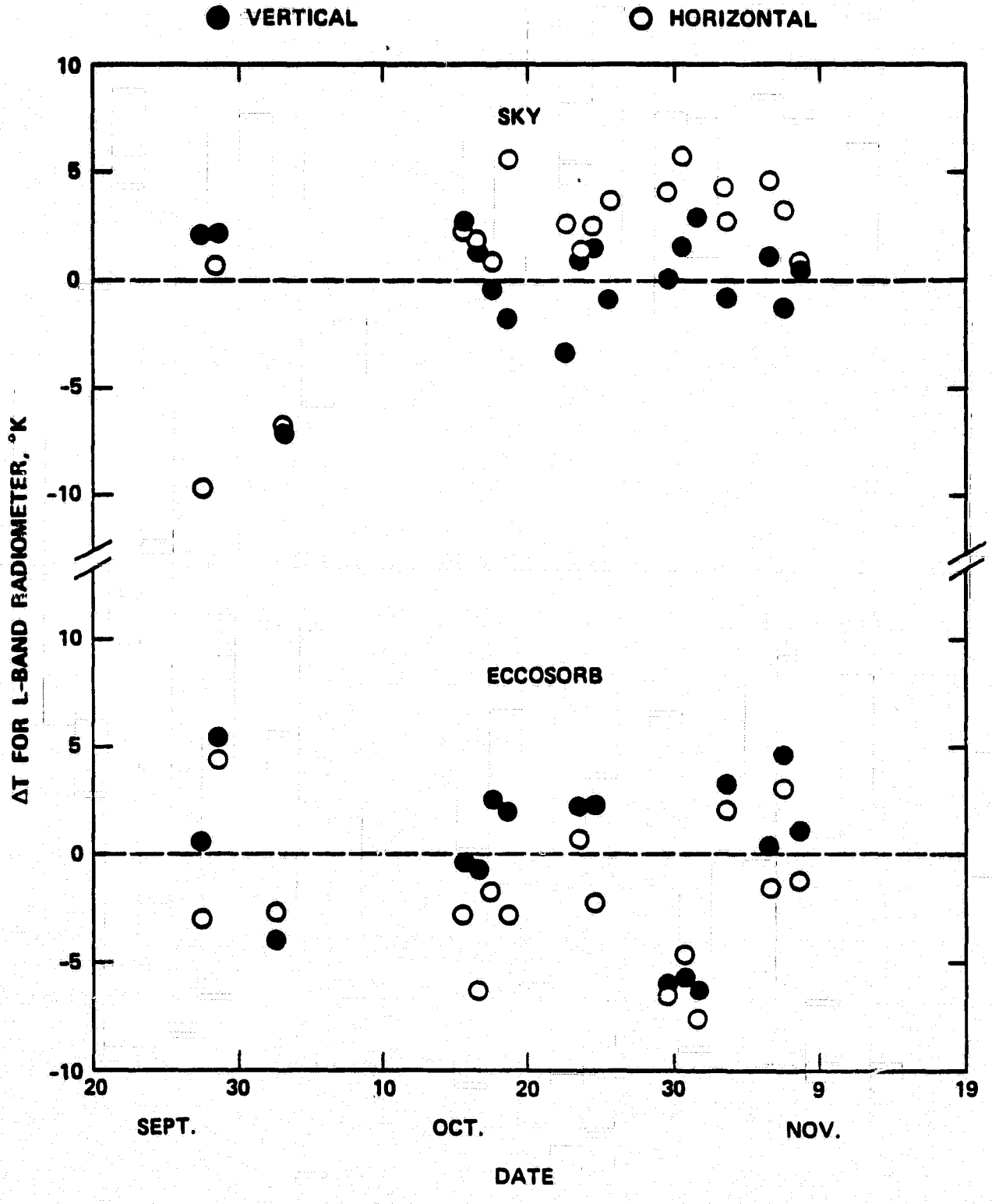


Figure 6. The difference between the measured and calculated L-band brightness temperatures for two calibration targets plotted as a function of time.

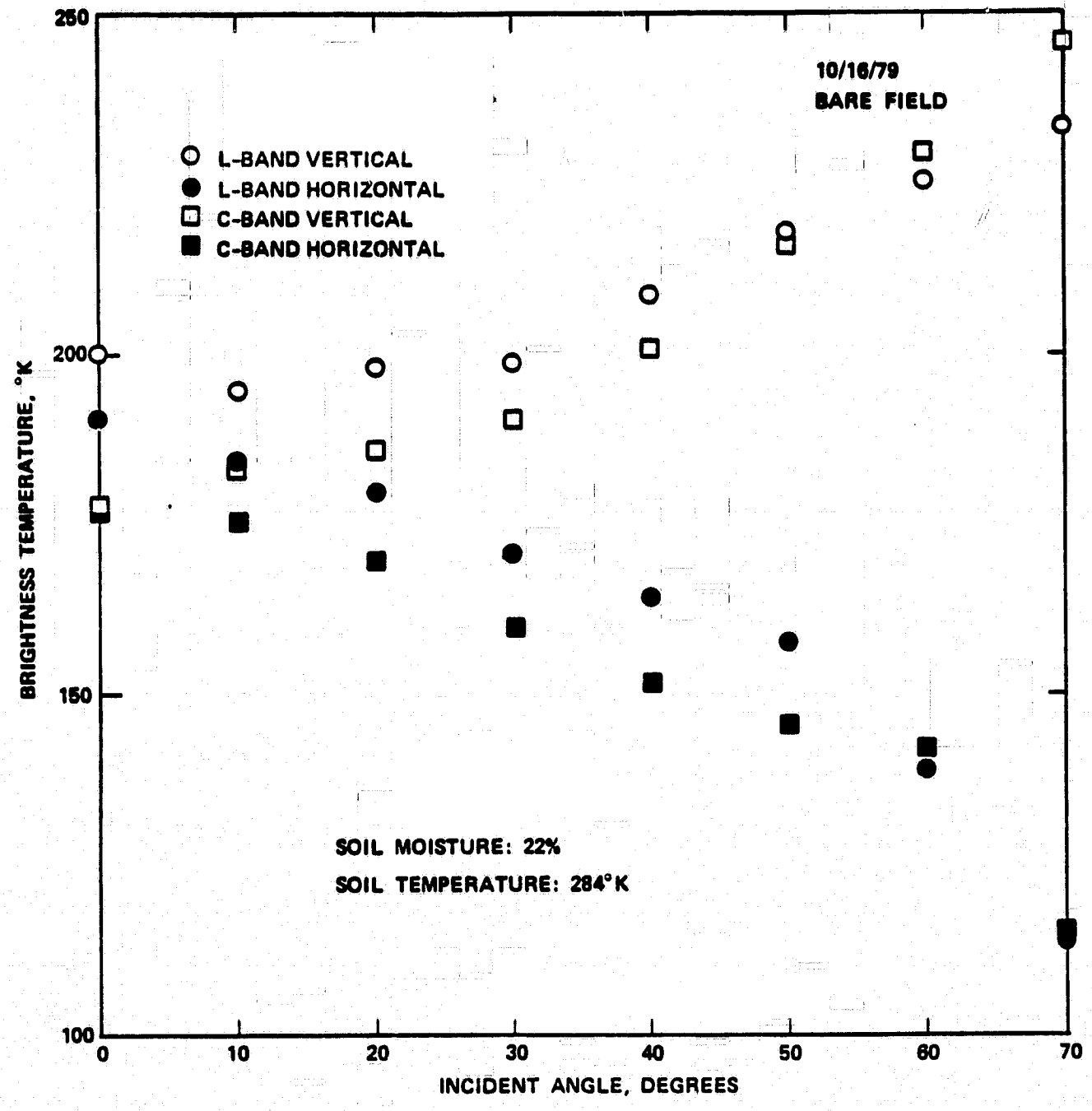


Figure 7. The measured C-band and L-band brightness temperatures as a function of incident angle over a bare field with uniform moisture content of ~22% down to 10 cm depth.

L-band by ~8°K or more at $\theta \leq 50°$K. Since the dielectric constant at C-band is expected to be comparable or smaller than that at L-band for a given soil moisture content, a radiative transfer model calculation for a uniform moisture profile would generally give an L-band $T_B \leq$ a C-band $T_B$. The data set in Figure 7 is not the only one which shows a lower $T_B$ for C-band than L-band over a bare field. Figure 8 shows a plot of the C-band versus L-band $T_B$'s at $\theta = 10°$ for all the 1979 measurements over the three bare fields. The majority of the data points were below the 1:1 line suggesting the generally lower C-band $T_B$'s compared to those of L-band. The two data points (open circles) above the line are the measurements over the bare field where the top 0 – 0.5 cm soil moisture content is ~5%. The sampling depth at C-band is expected to be smaller than that at L-band. Consequently, the C-band radiometer sensed the drier portion of the soil and the measured $T_B$'s were expected to be higher than those at L-band in these cases.

At the completion of the field measurements, an experimental test was made where the vertically polarized feed of the C-band antenna was replaced by a C-band horn so that both the horn and the phase array observed only the horizontally polarized radiation. The results of measurements with $\theta$ ranging from 10° to 70° for all bare fields were shown in Figure 9. With the exception of one set of measurements, $T_B$'s measured with phased array antenna were lower than those measured with horn antenna by ~2° – 5°K.

The evidences presented in Figures 7 through 9 strongly suggest that the C-band measurements in 1979 may have a bias problem. Whereas, the L-band radiometer could provide the radiometric measurements to an accuracy of ~ ±3°K based on the results shown in Figures 4 through 6, the C-band radiometric measurements over bare fields generally give lower values for $T_B$ by ~8°K (compared to L-band). The most likely source causing this bias problem is the C-band antenna radiation

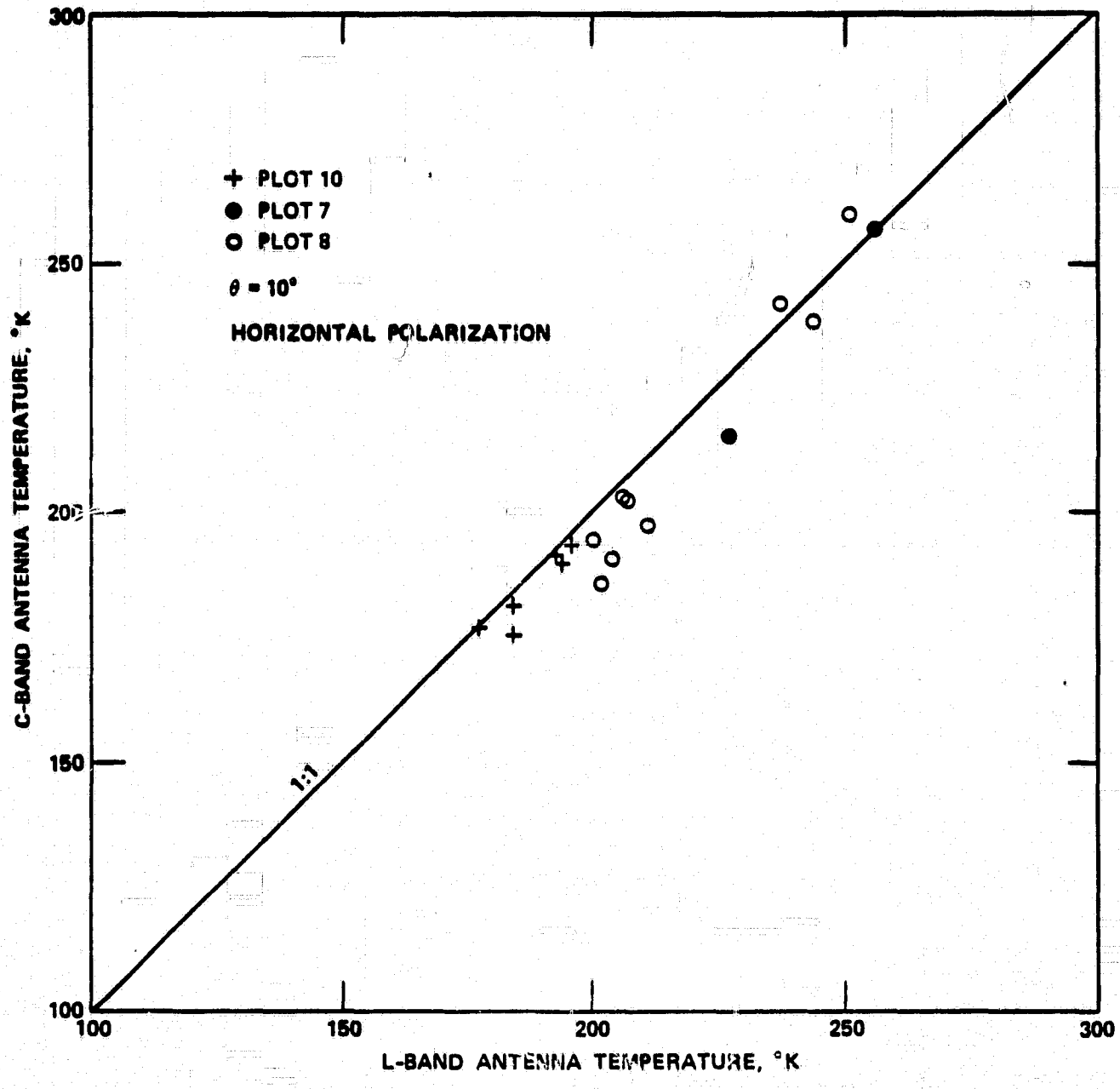


Figure 8. A comparison of measured C-band and L-band brightness temperatures (horizontal polarization) at 10° incident angle over bare fields. The field layout was given in Wang et al. (1980).

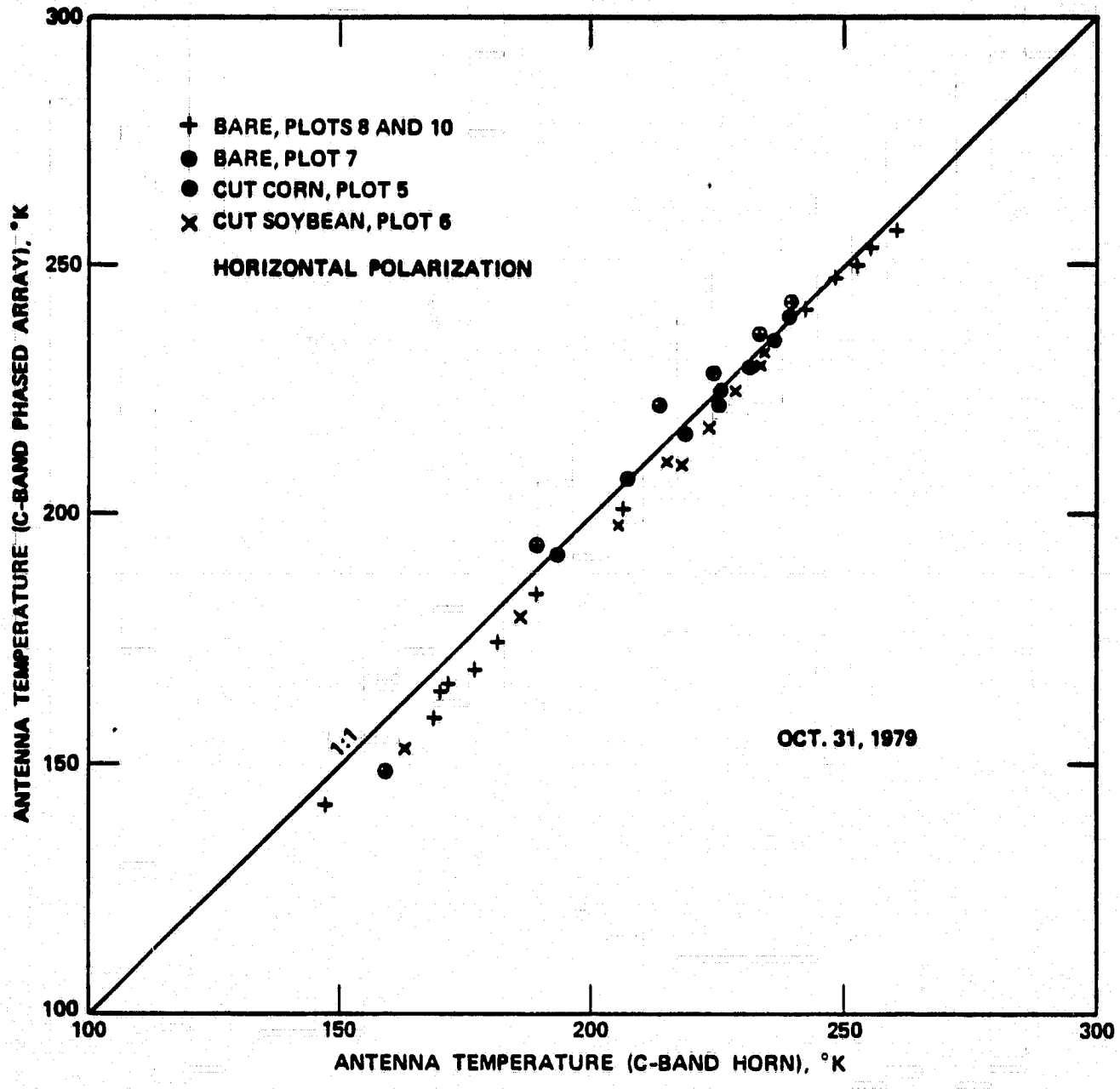


Figure 9. A comparison of brightness temperatures measured with C-band phased array antenna and with C-band horn over bare fields. The field layout was given in Wang et al. (1980).

pattern. As noted in Figure 2, the C-band phased array antenna possesses a significant side lobe at ~85° away from the main beam. For $\theta \geq 10°$ in the field measurements, that side lobe points to the sky and observes the cold brightness temperature of 5°K. It is difficult to estimate the contribution of the side lobe effect in the radiometer output without multiple-cut measurements of the radiation pattern.

Another factor which may give a lower brightness temperature at C-band than at L-band is the surface roughness effect. The surface roughness effect has been studied by Choudhury et al. (1979) in some detail. For a given soil moisture content, a rougher surface generally gives a higher brightness temperature. If the surface roughness effect is smaller at C-band than at L-band, then the brightness temperature measured at C-band can be lower than that at L-band for a given uniform soil moisture profile. Radar study by Ulaby and Batlivala (1976) shows that backscattering coefficient at $\theta = 10° - 20°$ and at C-band frequency is least dependent on the surface roughness effect. The same phenomenon may exist in the thermal microwave emission from a soil. Radiometric measurements at several frequencies over many different surface roughnesses are needed in order to determine the frequency dependence of surface roughness effect.

## 5. THE EFFECT OF ANTENNA SELF-EMISSION

It was observed (Carver, 1978 and Newton, personal communication) from measurements by radiometers mounted on a mobile tower that at $\theta = 0°$ the measured $T_B$ was higher than expected and the extra power appeared to come from the backscattered self-emission of the radiometer systems. Carver (1978) performed an experiment of this effect over a smooth water surface and found that the observed $T_B$ was proportional to $h^{-1/2}$, h being the height above the water surface. To test out this effect in our radiometer systems, an experiment was performed over the same water pond

used for system calibration described in Section 3. The radiometric measurements were made for $\theta = 0°, 10°, 20°$, and $40°$ with h varying from 0.61 m to 6.1 m in 10 steps. The results of these measurements were shown in Figures 10 and 11 for both C-band and L-band radiometers. The C-band results for $\theta = 20°$ and $40°$ showed no contribution from the radiometer's self-emission down to 0.61 m and were therefore omitted in the figures.

It is clear from these figures that the effect of self-emission for both C- and L-band radiometers is definitely present. For L-band radiometers, the effect can be observed even at $\theta = 20°$ and $h \leq 2$ m. The decrease of $T_B$ with h for both radiometers was not as rapid as that reported by Carver (1978). However, it can be shown that for $\theta = 0°$ and after contribution from water emission is subtracted, the residual $T_B$ is approximately proportional to $h^{-\frac{1}{2}}$ over the h range of 1.2 m to 6.1 m.

During the field measurements, the radiometers at $\theta \leq 30°$ were maintained at ~6 m above the ground. On the basis of the data presented in Figures 10 and 11, all the field radiometric measurements at $\theta \geq 10°$ should be free from the contamination of the radiometer self-emission. For $\theta = 0°$ the effect of radiometer self-emission is still present at h = 6 m and is difficult to correct because the reflectivity from surface depends on so many factors. Consequently, all the data obtained at nadir incidence should not be used for data analysis or interpretation.

## 6. CONCLUSIONS

Based on the radiometer system performance and data analysis presented in the previous sections, we have arrived at the following conclusions:

a. The L-band radiometer system appears to be in good shape. The accuracy of the radiometric measurements is estimated to be ~ ±3°K.

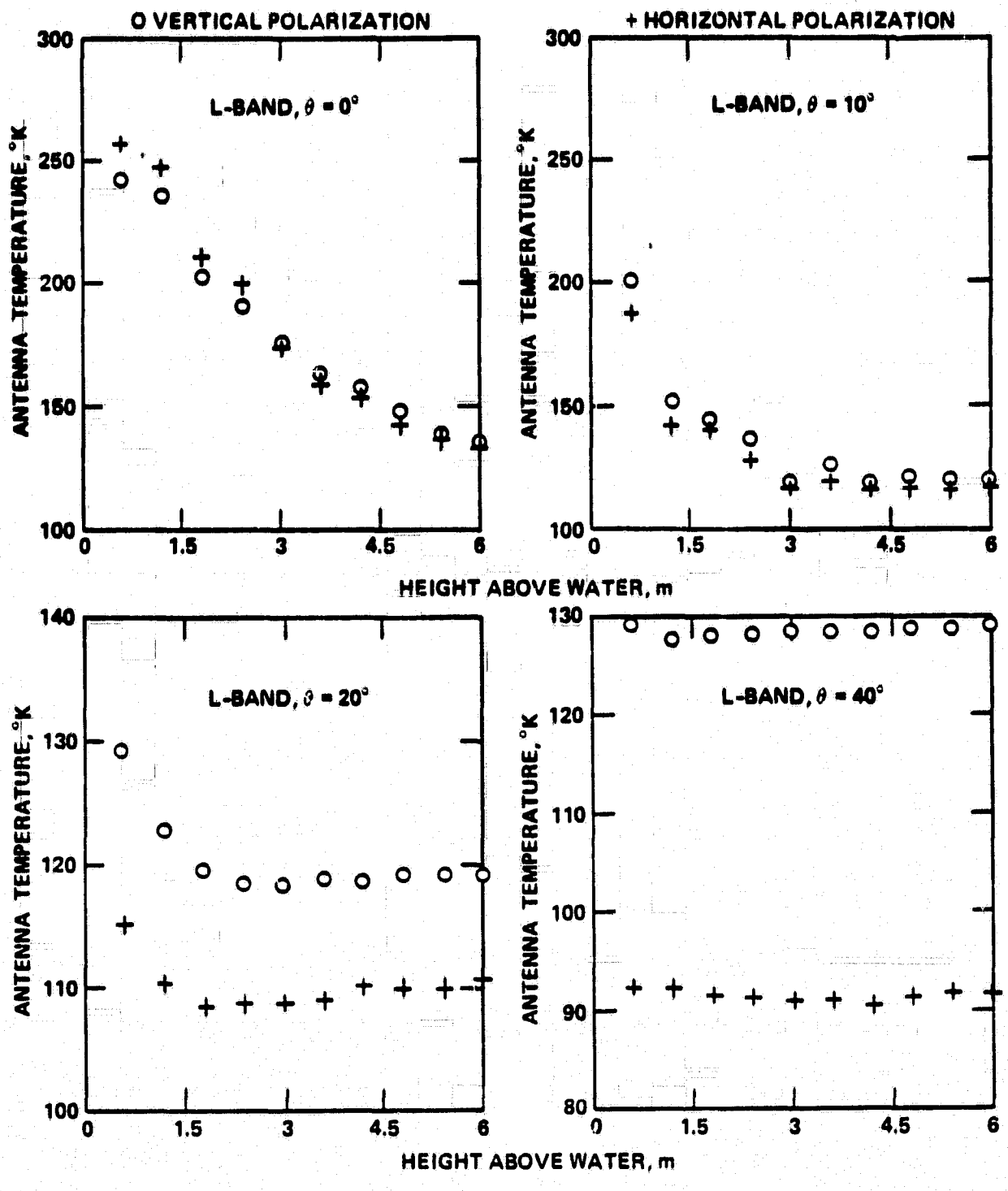


Figure 10. The measured L-band brightness temperatures as a function of height above a smooth water surface. The measurements were made at incident angles of 0°, 10°, 20°, and 40°.

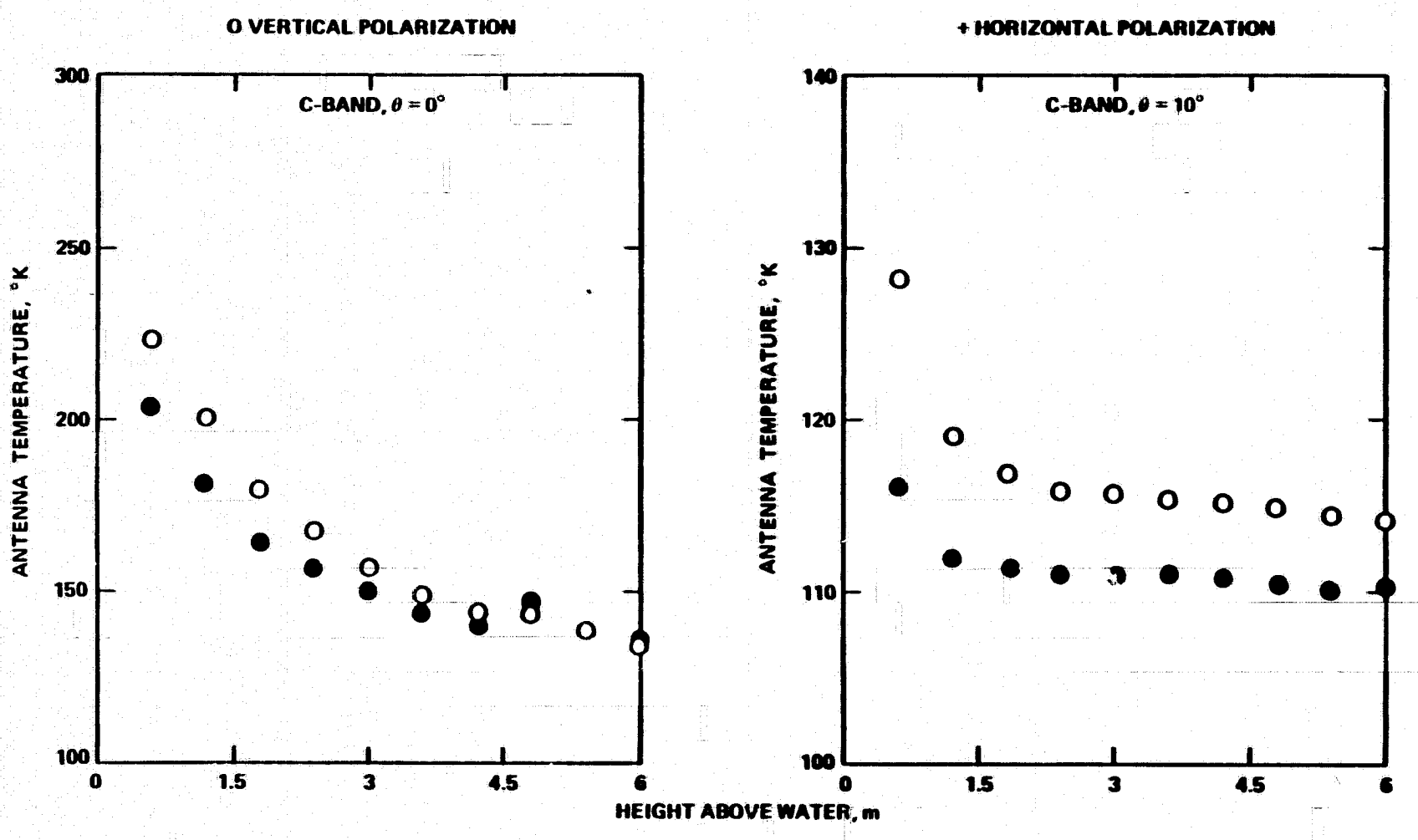


Figure 11. The measured C-band brightness temperatures as a function of height above a smooth water surface. For incident angles ≥20°, the effect of the radiometer self-emission (not shown here) is negligible.

b. The effect of radiometer self-emission on the radiometric measurements for both C- and L-band radiometers is definitely present. At incident angle $\theta = 0°$, the measured data are of questionable quality. For $\theta \geq 10°$, the measurements should be free from the effect of radiometer self-emission.

c. The C-band measurement results showed a bias of about -8° in brightness temperatures compared to L-band results. This is likely due to a significant side lobe at ~85° away from the main beam in the C-band antenna radiation pattern. In the future experiment, the C-band phased array antenna will be replaced. Another factor which should be considered in the future measurement program is the frequency dependence of the surface roughness effect. If the thermal microwave emission from a soil is less affected by surface roughness at C-band than at L-band frequency, then the brightness temperature observed at C-band can be lower than that at L-band for a given uniform soil moisture profile.

## REFERENCES


Carver, K. R., An experimental investigation of self-emission from microwave radiometers, International Union of Radio Science Spring Meeting, College Park, Md., p. 135, 1978.

Lane, J. A., and J. A. Saxton, Dielectric dispersion in pure polar liquids at very high radio frequencies. measurements on water, methyl and ethyl alcohols, *Proc. Roy. Soc., Vol. A213*, 400-408, 1952.

Newton, R. W., Joint soil moisture experiment at Texas A&M University, June 26 – July 21, 1974, Technical report RSC-65, Remote Sensing Center, Texas A&M University, College Station, Texas, 1975.

Newton, R. W., and E. A. Tesch, Joint soil moisture experiment ground based measurements at Texas A&M University, July 13 – July 25, 1975, Technical Report RSC-71, Remote Sensing Center, Texas A&M University, College Station, Texas, 1976.

Njoku, E. G., and J. A. Kong, Theory for passive microwave remote sensing of near surface soil moisture, *J. Geophys. Res.*, *82*, 3108-3117, 1977.

Paris, J. F., Microwave radiometry and its application to marine meteorology and oceanography, Ref. No. 69-1T, Texas A&M University, College Station, Texas, 1969.

Ulaby, F. T., and P. P. Batlivala, Optimum radar parameters for mapping soil moisture, *IEEE Trans. Geosci. Electron.*, Vol. GE-14, 81-93, Apr. 1976.

Wang, J., J. Shiue, E. Engman, J. McMurtrey, III, P. Lawless, T. Schmugge, T. Jackson, W. Gould, J. Fuchs, C. Calhoon, T. Carnahan, E. Hirschmann, and W. Glazar, Remote measurements of soil moisture by microwave radiometers at BARC test site, NASA TM 80720, AgRISTARS SM-GO-00471, October, 1980.

## FIGURE CAPTIONS

Figure 1. The measured radiation pattern for the L-band dish antenna (vertical polarization).

Figure 2. The measured radiation pattern for the C-band phased array antenna (vertical polarization).

Figure 3. The C-band calibration data and results.

Figure 4. The L-band calibration data and results.

Figure 5. The difference between the measured and calculated C-band brightness temperatures for two calibration targets plotted as a function of time.

Figure 6. The difference between the measured and calculated L-band brightness temperatures for two calibration targets plotted as a function of time.

Figure 7. The measured C-band and L-band brightness temperatures as a function of incident angle over a bare field with uniform moisture content of ~22% down to 10 cm depth.

Figure 8. A comparison of measured C-band and L-band brightness temperatures (horizontal polarization) at 10° incident angle over bare fields. The field layout was given in Wang et al. (1980).

Figure 9. A comparison of brightness temperatures measured with C-band phased array antenna and with C-band horn over bare fields. The field layout was given in Wang et al. (1980).

Figure 10. The measured L-band brightness temperatures as a function of height above a smooth water surface. The measurements were made at incident angles of 0°, 10°, 20°, and 40°.

Figure 11. The measured C-band brightness temperatures as a function of height above a smooth water surface. For incident angles $\geq 20°$, the effect of the radiometer self-emission (not shown here) is negligible.